Different patterns of apoptosis in response to cisplatin in B50 neuroblastoma rat cells

G. Santin[1], V.M. Piccolini[1], P. Veneroni[1], S. Barni[3], G. Bernocchi[1,2] and M.G. Bottone[1,2]

[1]Department of Animal Biology, Laboratory of Cell Biology and Neurobiology, University of Pavia, Pavia, Italy, [2]CNR Institute of Molecular Genetics, Histochemistry and Cytometry Section, University of Pavia, Pavia, Italy and [3]Department of Animal Biology, Laboratory of Comparative Anatomy and Cytology, University of Pavia, Pavia, Italy

Summary. Cisplatin (cisPt) is a chemotherapeutic drug used for several human malignancies. CisPt cytotoxicity is primarily mediated by its ability to cause DNA damage and subsequent apoptotic cell death. DNA is the primary target of cisPt; however, recent data have shown that cisPt may have important direct interactions with mitochondria, which can induce apoptosis and may account for a significant part of the clinical activity associated with this drug. We have previously demonstrated that in the rat neuronal cell line B50, at 20 h-treatment with cisPt activates apoptosis through an intrinsic pathway involving an alteration of mitochondrial membrane permeability and the release of cytochrome c. The present study investigates different death pathways induced in the same cell line by a prolonged treatment with 40 μM cisPt for 48 h. To address this issue, we focused on caspases-8 and -12, and on the mitochondrial apoptosis inducing factor (AIF), which translocates to the nucleus and induces cell death via caspase-independent pathway. We found that cisPt activates different forms of cell death, i.e. the receptor-mediated apoptotic extrinsic pathway and a death process mediated by endoplasmic reticulum stress. Moreover, we demonstrated that AIF-mediated death occurs, being characterized by the translocation of AIF from mitochondria to the nucleus. On the whole, we provided evidence that prolonged cisPt treatment is able to activate both caspase-dependent and caspase-independent apoptotic pathways in B50 rat neuronal cells.

Key words: B50 neuroblastoma rat cells, Apoptosis, Cisplatin, Mitochondria, Endoplasmic reticulum

Introduction

Cisplatin (cisPt) represents a unique and important class of antitumor agents, widely used for the treatment of many malignancies, including testicular, ovarian, bladder, cervical, head and neck, small-cell and non-small-cell lung cancers (Rosenberg, 1999). It is generally accepted that DNA damage and subsequent induction of apoptosis may be the primary mechanism of cisPt toxicity (Fisher, 1994).

Apoptosis is a conserved cell-death process displaying morphological and molecular characteristic features. It is important for sculpting tissues and destroying harmful cells such as autoreactive immune cells and tumor cells (Abraham and Shaham, 2004). Features of apoptosis include surface membrane blebbing, dilatation of the endoplasmic reticulum, externalization of phosphatidylserine at the cell surface, nuclear and cytoplasmatic condensation and DNA fragmentation. Most, if not all, of these phenomena are induced by caspases in the apoptosis "execution" phase. Caspases belong to a cysteine protease family that cleaves critical intracellular substrates at key aspartate residues, thereby activating apoptosis (Kruiderin and Evan, 2000).

We have already demonstrated that mitochondria represent one of the main targets of anticancer chemotherapy. In fact, after cisPt treatment of neuroblastoma rat cells (B50), we found that apoptosis is triggered through the intrinsic pathway mediated by the alteration of mitochondrial membrane permeability, which entails the formation of a transition pore (MPTP, Membrane Permeability Transition Pore) and the release into the cytosol of proteins stimulating apoptosis (Bottone et al., 2008). One of the most important proteins involved is cytochrome c, which forms a complex named *apoptosome* and activates caspase-9; caspase-9, in turn, activates caspase-3, which leads the

cell to death (Kaufmann, 2007).

AIF (Apoptosis Inducing Factor) is another protein released from mitochondria and involved in the caspase-independent apoptotic pathway: it moves from the mitochondria to the nucleus where it mediates chromatin condensation and large-scale DNA fragmentation, possibly by binding to DNA (Modjtahedi et al., 2006), then it moves back to the cytoplasm (Bottone et al., 2010). There is a strong, positive, electrostatic potential at the surface of the AIF protein, which indicates that this protein might bind to DNA: AIF recruits proteases and nucleases, such as endonuclease G, which causes chromatin condensation (Zhang et al., 2007). Recently, it has been shown that AIF is implicated in different neurodegenerative disorders and that this molecule can be a trigger of cell death (Camins et al., 2008; Perier et al., 2010).

Caspase-8 is one of the crucial molecules for cell death induction, especially *via* "death-receptor pathway" (Barnhart et al., 2003); furthermore, even when caspase-8 may not be absolutely required for apoptosis, it can clearly act to accelerate apoptosis, presumably through its recruitment by other caspases. Altered expression or function of caspase-8 can promote tumor formation, progression and treatment resistance in several types of cancers (Fulda, 2008). The precursor of this caspase (procaspase-8) is sequestered into an oligomeric activating complex; the assembled Fas-FADD-caspase-8 complex is known as the death-inducing signaling complex (DISC) (Kruiderin and Evan, 2000). Activated caspase-8 can initiate a strong proteolysis by processing caspase-3 directly (Adams, 2003).

Stress to the endoplasmic reticulum (ER) produced by disturbed glycosylation, misfolded proteins, perturbed calcium homeostasis or glucose deprivation provokes the unfolded protein response, and the persistence of this response induces apoptosis (Ferri and Kroemer, 2001) through the activation of caspase-12, a cystein protease that resides on the cytoplasmic district of the ER and that is activated by ER stress (Nakagawa et al., 2000). Caspase-12, during apoptosis, is responsible for caspase activation cascade and finally, like caspase-9 and caspase-8, activates caspase-3.

In the present study, we investigated if cisPt, induces both caspase-dependent and caspase-independent apoptosis associated with caspase activation and mitochondrial AIF traslocation, respectively. The study was carried on rat B50 neuroblastoma rat cells submitted to continuous exposure to a single dose of cisPt (40 μM) for 20 h and 48 h.

Materials and methods

Cell culture and treatments

Neuroblastoma rat B50 cells (ATCC, USA) were grown in 75 cm^2 flasks in D-MEM supplemented with 10% fetal bovine serum, 1% glutamine, 100 U of penicillin and streptomycin (Celbio, Italy) in a 5% CO$_2$ humidified atmosphere. 24 hours before the experiments, cells were seeded on glass coverslips for fluorescence microscopy or grown in 75 cm^2 plastic flasks for flow cytometric analysis.

To induce apoptosis, the cells were incubated with 40 μM cisPt (Teva Pharma, Italy) for 48 h at 37°C. This concentration was chosen considering our in vivo experimental design (i.e. a single injection of 5 μg/g in 10-day-old rats). This concentration corresponds to the dose most commonly used in the chemotherapy (Bodenner et al., 1986; Dietrich et al., 2006).

Identification of apoptotic cells in flow cytometry

Cells were detached by mild trypsinization (to obtain single-cell suspensions to be processed for flow cytometry), washed in phosphate-buffered saline (PBS) and stained for 20 min at room temperature with 1 μg/ml Hoechst 33258 (Sigma Aldrich) 1 h before flow cytometric analysis.

DNA amount measurements were taken by a Partec PAS III flow cytometer (Münster) equipped with a 100W mercury lamp. At least 20000 cells/sample were measured; five independent experiments were carried out and the average score was used.

Values are expressed as the mean ± SEM and differences were compared using Student's *t*-test.

Identification of apoptotic cells with annexin V/FITC versus Propidium Iodide (PI)

Cells were detached by mild trypsinization as before, incubated with FITC-conjugated annexin V (3 μL/10^6 cells) (Bender MedSystem, Prodotti Gianni) and counterstained with 2 μg/ml PI. After 10 min incubation, dual parameter flow cytometric analysis was performed with the flow cytometer Partec PAS III, equipped with argon laser excitation (power 200 mW) at 488 nm, 510–540 nm interference filter for the detection of FITC green fluorescence, and a 610 nm long-pass filter for PI red fluorescence detection. Five independent experiments were carried out and the average score was used. Values are expressed as the mean ± SEM and differences were compared using Student's *t*-test.

Immunocytochemical staining for activated caspase-8 and caspase-12

Cells on coverslips were fixed with acetone for 10 min, rehydrated with PBS and incubated with primary polyclonal antibodies recognizing the active form of caspase-8 (Cell Signaling, Celbio, Italy, diluted 1:50 in PBS) or the active form of caspase-12 (Cell Signaling, diluted 1:50 in PBS), in a humidified chamber for 1 h at room temperature. Then, cells were washed with PBS and incubated with Alexa 488-conjugated anti-rabbit antibody (Molecular Probes, Invitrogen, Italy, diluted 1:200 in PBS); slides were finally incubated with 1 μg/mL PI for 5 min at room temperature, washed with

PBS and then mounted with Mowiol (Calbiochem, Inalco, Italy) for confocal microscopy analysis. Three independent experiments were carried out and the average score was used. Values are expressed as the mean ± SEM and differences were compared using Student's *t*-test.

Double immunocytochemical detection of AIF and mitochondria

After the treatments, the samples were fixed with 4% formalin and post-fixed with 70% ethanol for 24 h at -20°C. Samples were permeabilized for 15 min in PBS and then immunolabelled with one of the following antibodies: polyclonal antibody recognizing AIF (Cell Signaling, diluted 1:100 in PBS); monoclonal antibody recognizing the mitochondrial isoform of HSP70 (Alexis, Italy, diluted 1:50 in PBS). The incubation with the primary antibody was followed by the incubation with either Alexa488-conjugated anti-mouse or Alexa594-conjugated anti-rabbit IgGs (Molecular Probes, Invitrogen, Italy, diluted 1:200 in PBS). As a negative control, parallel samples were incubated without the primary antibodies, and finally exposed to the appropriate secondary antibody. All the incubations were performed at room temperature for 1 h and cells were finally counterstained for DNA with 0.1 μg/ml of Hoechst 33258 for 10 min, washed with PBS, and mounted with Mowiol for conventional and confocal microscopy.

Immunocytochemical staining for endoplasmic reticulum

After the treatments, the samples were fixed with 4% formalin and post-fixed with 70% ethanol for 24 h at -20°C. Samples were incubated with polyclonal GRP94 antibody - ER Marker (ab3674-Abcam, UK, diluted 1:50 in PBS), and revealed with Alexa 594-conjugated anti-rabbit antibody (Molecular Probes, diluted 1:200 in PBS). Incubations were performed for 1 h at room temperature. Samples were counterstained for DNA with 0.1 μg/mL Hoechst 33258, washed with PBS and mounted in Mowiol, for fluorescence microscopy or confocal microscopy analysis.

Isolation of mitochondria, nuclei and cytoplasm and western blotting analysis.

Western blotting was carried out after protein extraction: for caspases, cells are washed with a CoIP complete buffer (H_2O_d, Tris HCl pH 7.6 20 mM, EDTA pH 8.0 10 mM, NaCl 280 mM, Nonidet NP40, Proteases Inhibitor 1% and Na_3Vo_4 2 mM), for AIF and cytochrome c the isolation of mitochondrial and nuclear subcellular fraction was made with Mitochondrial Isolation Buffer (Mannitol 200 mM, Sucrose 70 mM, EGTA 1 mM, Hepes 10 mM and Protease Inhibitor) and Nuclear Isolation Buffer A (Hepes pH 7.9 10 mM, KCl 10 mM, EDTA 0.1 mM, DTT 1 mM and PMSF 0.5 mM) and Buffer C (Hepes pH 7.9 20 mM, NaCl 0.4 M, EDTA 1 mM, DTT 1 mM, PMSF 1 mM and Protease inhibitor 1%) (Sigma Aldrich, Italy).

Samples were electrophoresed in a 10% or 12% SDS-PAGE minigel and transferred onto a nitrocellulose membrane (BioRad, Hercules, CA) by a semidry blotting for 1.45 h under a constant current of 70 mA. The membranes were incubated overnight with the primary antibodies (anti-mtHSP70 Alexis 1:500, anti-histone H3 Cell Signaling 1:1000, anti-caspase-3 Cell Signaling 1:1000, anti-caspase-8 Cell Signaling 1:1000, anti-caspase-12 Cell Signaling 1:1000, anti-cytochrome c Cell Signaling 1:1000, anti-AIF Cell Signaling 1:1000, anti-ß-tubulin III Molecular Probes 1:25000). After several washings, the membranes were incubated for 30 min with the proper secondary antibodies conjugated with horseradish peroxidase (Dako, Italy), then they were washed and revealed using enhanced chemiluminescence (Amersham).

Fluorescence microscopy

An Olympus BX51 microscope equipped with a 100W mercury lamp was used under the following conditions: 330-385 nm excitation filter (excf), 400 nm dichroic mirror (dm), and 420 nm barrier filter (bf) for Hoechst 33258; 450-480 nm excf, 500 nm dm and 515 nm bf for the fluorescence of Alexa 488; 540 nm excf, 580 nm dm, and 620 nm bf for Alexa 594. Images were recorded with an Olympus MagniFire camera system and processed with the Olympus Cell F software.

Fluorescence confocal microscopy

For confocal laser scanning microscopy, we used a Leica TCS-SP system mounted on a Leica DMIRBE inverted microscope; for fluorescence excitation, an Ar UV laser at 364 nm was used for Hoechst 33258, Ar visible laser at 488 nm for Alexa 488 and He/Ne laser at 543 for Alexa 594. Spaced (0.5 μm) optical sections were recorded using a 63x oil immersion objective. Images were collected in the 1024x1024 pixels format, stored on a magnetic mass memory and processed by the Leica Confocal Software.

Transmission electron microscopy (TEM)

For TEM, the cells were harvested by mild trypsinization (0.25% trypsin in PBS containing 0.05% EDTA), immediately fixed with 2% glutaraldehyde in the culture medium (1 h at 4°C) and post-fixed in 1% O_sO_4 in PBS for 1 h at r.t. The cell pellets were embedded in 2% agar, thoroughly rinsed with Sörensen buffer (pH 7.2) and dehydrated in ethanol. Finally, the pellets were embedded in LR White resin and polymerized at 60°C for 24 h. Ultrathin sections were stained with uranyl acetate and lead citrate, and observed
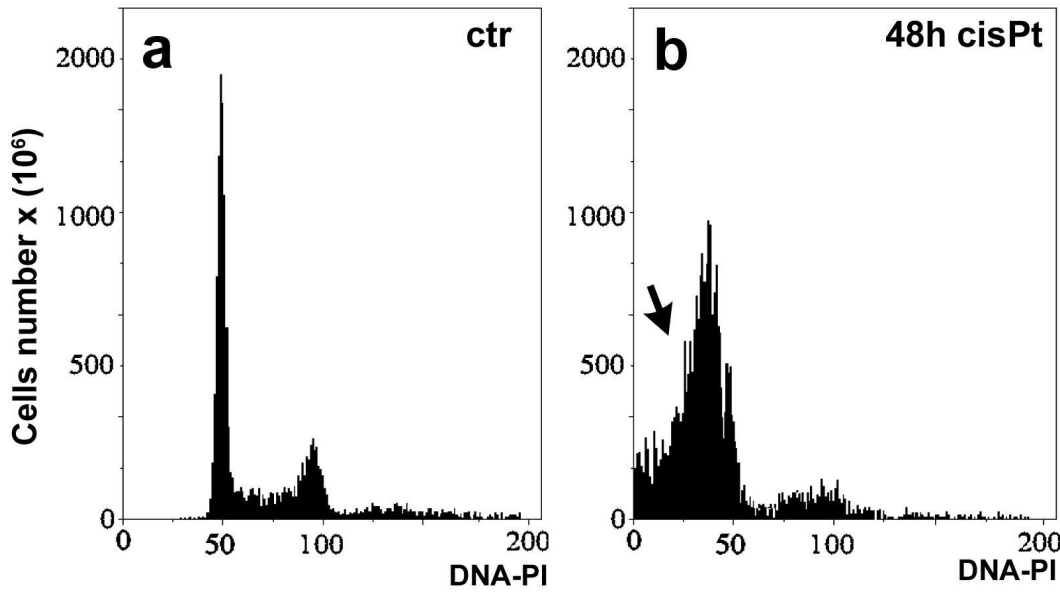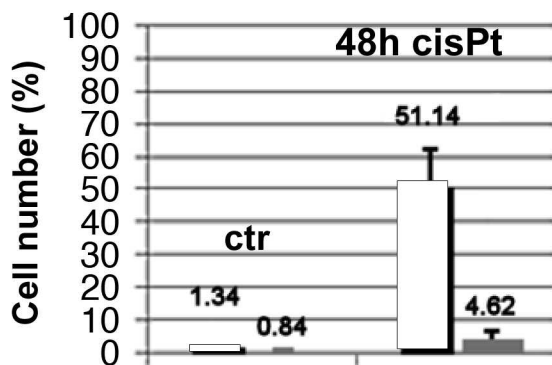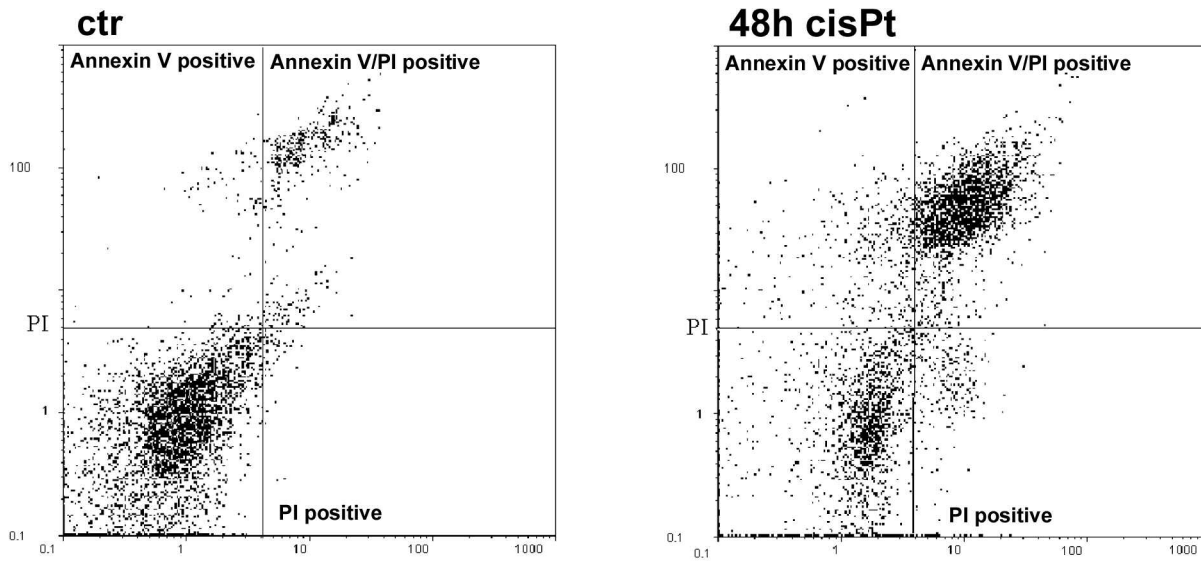
Fig. 1. DNA amount measured by flow cytometry. **a.** Control B50 cells. **b.** Cells treated for 48 h with 40 μM cisPt. Arrow: apoptotic fraction.

Fig. 2. Biparametric analysis with Annexin V/FITC versus PI in control and 48 h cisPt treated cells. Graphics above shows early (Annexin V positive) and late (Annexin V and PI positive) apoptotic cells. The bar chart reveals the apoptotis percentage increase after treatment.

under a Zeiss EM900 transmission electron microscope.

Results

Evaluation of DNA content and apoptosis in Flow Cytometry

We evaluated cisPt apoptotic effect in B50 48 h cisPt (40 μM) treated cells, after a previous work with B50 20 h cisPt treated samples (Bottone et al., 2008). In comparison with the control situation, in which the percentage of spontaneous apoptosis is about 2±0.1% (Fig. 1a), a relevant apoptotic effect is recognizable after 48 h of cisPt (41±2,1%) (Fig. 1b). This suggests that, already at 20 h post treatment samples are affected by cisPt activity (Bottone et al., 2008), but the effect became more relevant with longer exposure time.

Identification of apoptotic cells with Annexin V/FITC versus Propidium Iodide (PI)

Appearance of phosphatidylserine residues (normally hidden within the plasma membrane) on the surface of the cell is a parameter that can be used to detect and measure apoptosis since cell membrane integrity is lost as the apoptotic process progresses. Using DNA-specific viability dyes, such as PI, it is possible to distinguish early apoptotic cells (Annexin V-positive cells) and late apoptotic cells (Annexin V- and PI-positive cells). We already carried out the experiment on 20 h-treated samples (Bottone et al., 2008), where there was an increase in the early and late apoptotic cells. In this work, experiments revealed that also after 48 h of cisPt treatment apoptotic cell percentage increases: early apoptotic fraction was 0.84±0.3% in controls and 4.62±0.9% in treated cells, while late apoptosis ranged from 1.34±0.7% to 51.14±2.1% in control and treated cells, respectively (Fig. 2).

Activation of mitochondrial apoptotic pathways

When apoptotic stimulus causes perturbation at mitochondrial membrane potential, there is the release into the cytoplasm of cytochrome c and AIF, which mediate the intrinsic caspase-dependent pathway and the intrinsic caspase-independent pathway, respectively.

Immunofluorescence confocal analysis revealed, in B50 untreated cells, a colocalization between AIF and mitochondrial isoform of HSP70, a mitochondrial protein involved in protein translocation into the mitochondria (Fig. 3). In comparison with a control situation (Fig. 4a, a'-star), in cisPt treated B50 cells there was an increase of AIF immunopositivity in the nucleus, although no apoptotic nuclei were visible (Fig. 4b, b'-triangle).

Western blotting experiments confirmed the relocation of AIF from mitochondria to the cytoplasm and then to the nucleus (Fig. 4): the 57 kDa band of AIF in mitochondrial subcellular fraction was visible in control samples and decreased after 48 h of cisPt, while in the nuclear subcellular fraction it decreased in controls and increased in 48 h treated cells.

We already investigated the activation of caspase-9 (mitochondrial intrinsic pathway) in cisPt treated samples (Bottone et al., 2008). Now, after western blotting analysis, we confirmed the release of cytochrome c from mitochondria: in fact, in mitochondrial subcellular fraction, after 48 h of cisPt treatment the 14 kDa band (visible in controls) disappeared (Fig. 4), thus indicating that cytochrome c was no longer present within mitochondria.

Spatial relationship between nuclear changes and AIF translocation from mitochondria to the nucleus were analyzed in the confocal optical section images. Figure 5a shows AIF localization in the nucleus in early apoptotic cells (star): the bar chart of fluorescence intensity reveals a fusion of red/blue fluorescence measured in the section of the same cell. Confocal images of late apoptotic cells (Fig. 5b) show that AIF was located in the cytoplasm, while no signal for AIF was recorded in the nucleus (triangle); accordingly, the bar chart of fluorescence intensity confirmed that there is no fusion of red/blue fluorescence measured in the section of the same cell.
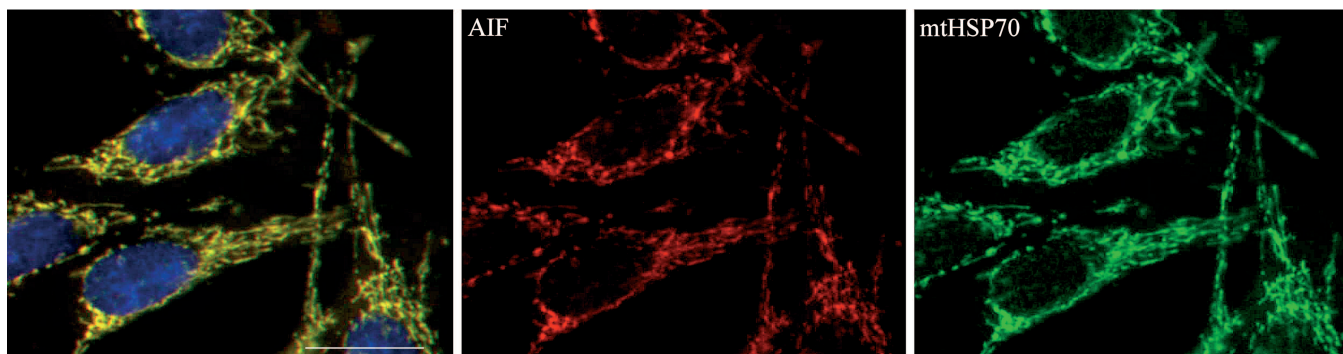

Fig. 3. Confocal microscopy. Dual immunolabelling for AIF (red fluorescence) and for the mitochondrial heat shock protein mtHSP70 (green fluorescence) in control B50 cells. DNA was counterstained with Hoechst 33258 (blue fluorescence). Red and green fluorescence overlap. Bar: 20 μm.
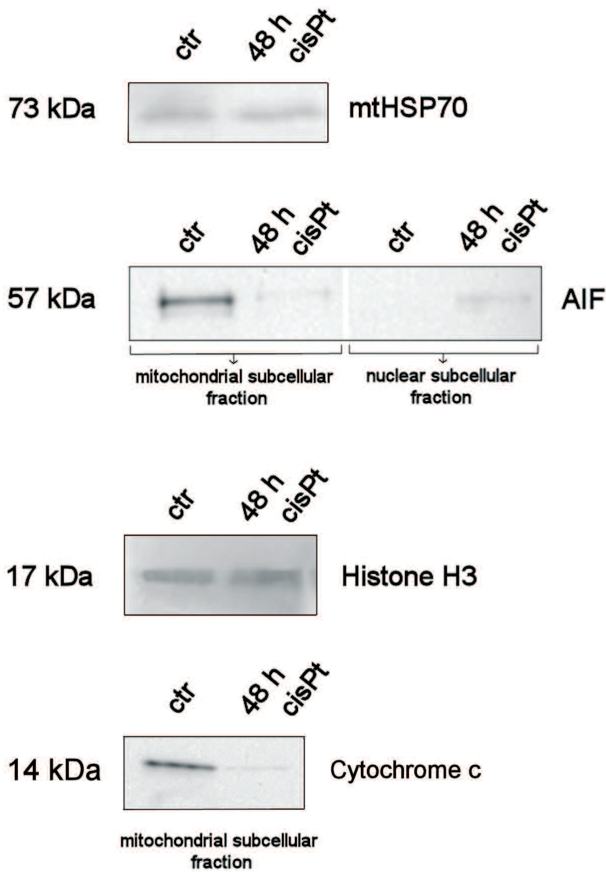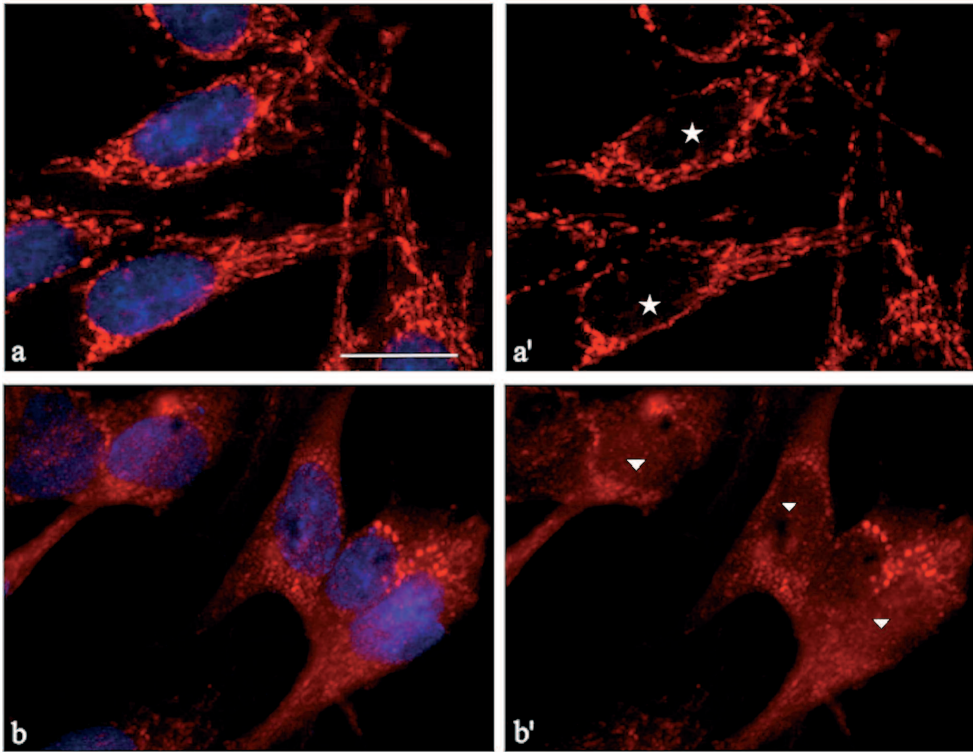
Fig. 4. Confocal microscopy. Immunolabelling for AIF. **a, a'.** Control cells, AIF (red fluorescence) is located in mitochondria and not in the nucleus (star). **b, b'.** cisPt treated cells, AIF moves into the nucleus (triangle). The cytoplasmic diffuse red fluorescence (in **b and b'**) suggest that AIF, before going into the nucleus, moves within the cytoplasm. DNA was stained with Hoechst 33258 (blue fluorescence). Western blotting analysis of AIF (57 kDa) after mitochondrial and nuclear subcellular fraction isolation. Western blotting of cytochrome c (14 kDa) in mitochondrial subcellular fraction. MtHSP70 is used as positive control for mitochondria; H3 histone is used as positive control for nucleus. Bar: 20 *μ*m.

Activation of extrinsic apoptotic pathway

Like all caspases, caspase-8 is synthesized as an inactive single polypeptide chain zymogen procaspase and it is activated by proteolytic cleavage, throughout either autoactivation after recruitment into a multimeric complex or trans-cleavage by other caspases. Activated caspase-8 is known to propagate the apoptotic signal by directly cleaving and activating downstream caspases (Kruiderin and Evan, 2000) and to be involved in the extrinsic pathway.

In comparison with control samples (Fig. 6a), a considerable increase in caspase-8 cytoplasmic immunopositivity was observed in cells after 48 h cisPt exposure (Fig. 6b). In fact, after this treatment the percentage of caspase-8 positive cells was 60±1.2%, while in control cells the percentage was 2.2±0.1%; this event was correlated to the activation of the apoptotic extrinsic pathway. This result is supported by western blotting analysis, which demonstrated that after 48 h of treatment the cleavage of procaspase-8 (55 kDa) in actived caspase-8 occurred (18 kDa) (Fig. 6).

Apoptotic pathway mediated by endoplasmic reticulum stress

Recent studies have identified the endoplasmic reticulum as a further subcellular compartment implicated in apoptotic execution when it is submitted to a stress condition. ER stress causes disruption of ER calcium homeostasis and accumulation of proteins in ER (Nakagawa et al., 2000). Caspase-12 is activated by ER stress and it specifically participates in ER stress-induced apoptosis (Rao et al., 2004). In fact, compared to a control situation (Fig. 7a), ER underwent a strong rearrangement in treated cells (Fig. 7b): the structure showed total disintegration and the cisternae were compressed in the cytoplasm with a non homogeneous distribution. Moreover, we analyzed protease expression; activation of caspase-12 was observed in cytoplasm of the cisPt treated cells (Fig. 7d). The percentage of caspase-12 positive cells was 43±2.3%, which is very high in comparison with the control situation (1.8±0.2%). Also, western blotting analysis reveals that caspase-12 undergoes activation: the 55 kDa precursor
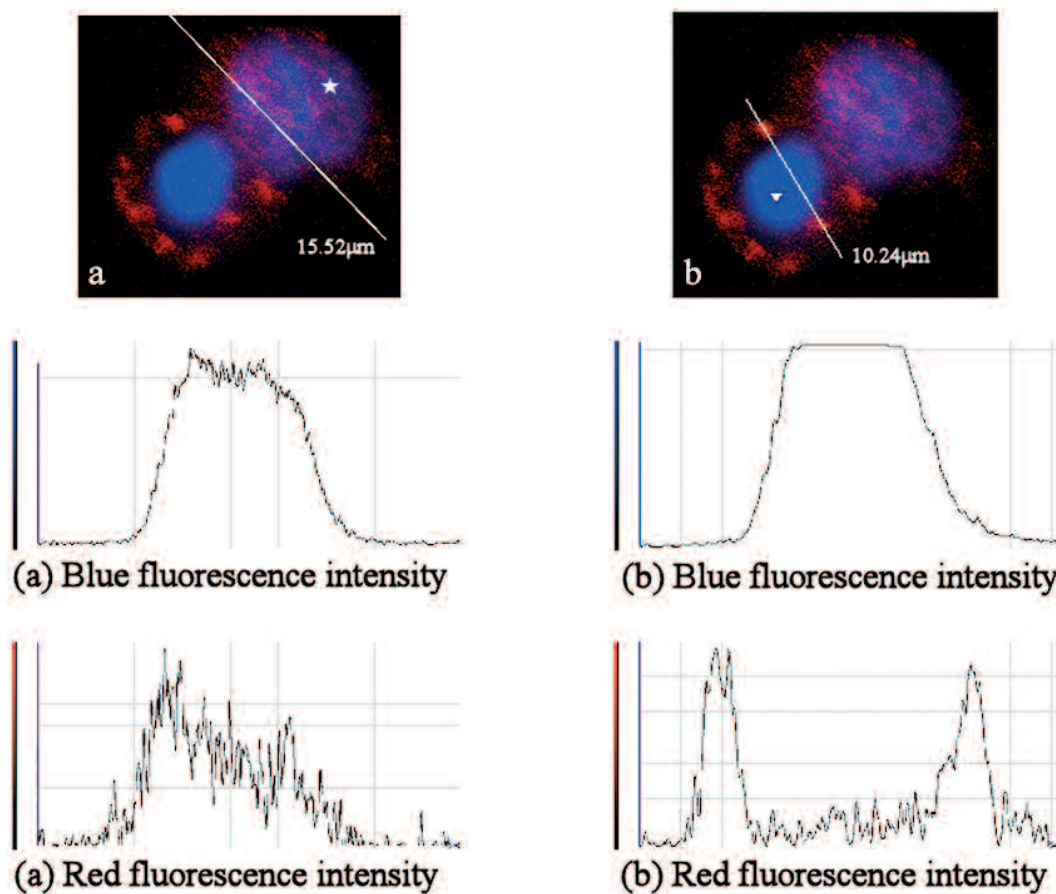

Fig. 5. Confocal optical sections after immunolabelling for AIF (red fluorescence) in early (**a**-star) and in late (**b**-triangle) apoptotic B50 cells after treatment with 40 μM cisPt for 48 h. DNA was stained with Hoechst 33258 (blue fluorescence). The upper bar chart is for blue fluorescence intensity (chromatin DNA) and the lower one for red fluorescence (AIF immunolabelling). In (**a**) blue and red peak coincide, in (**b**) they are different suggesting that there is no overlapping and that AIF is not nuclear.

enzyme is cleaved at 43 kDa in 48 h treated cells (Fig. 7). These results indicate that ER-associated caspase-12 plays an important role in cisPt-induced apoptosis.

In Figure 8, electron micrographs confirm that, as consequent of cisPt treatment, in apoptotic cells endoplasmic reticulum loses the physiological distribution in the cytoplasm (Fig. 8b, star) and results altered (Fig. 8d, arrows)

Western blotting analysis of executioner caspase-3

Caspase-3 is the executioner protease which is activated, as a final cascade step, in all the apoptotic caspase-dependent pathways, because it is the main effector of subcellular degradation followed by the formation of apoptotic bodies. In a previous work, we already described the activation of executioner caspase-3 through immunofluorescence analysis (Bottone et al., 2008). Now, caspase-3 western blotting analysis confirms the cleavage-mediated activation of the protease. In fact, after 48 h of cisPt treatment, the 19

kDa cleaved caspase was visible, while in control samples only the 35 kDa precursor band was detected (Fig. 9). This result supports previous data obtained with immunocytochemical analysis.

Discussion

It is known that neuroblastoma cells undergo apoptosis after cisPt treatment (Cece et al., 1995). In fact, cisPt has been used as a chemotherapeutic agent in many cancers, but the molecular mechanisms of its anti-cancer activity are not clear.

Previous experiments demonstrated that 20 h-cisPt treatment induced apoptosis (Bottone et al., 2008); now we demonstrated that after 48 h of treatment the same result is obtained. Initially, it is confirmed by the DNA amount measured by flow cytometry: in control sample there is a very small spontaneous apoptosis portion, but after 48 h of treatment there is a strong increase of apoptotic percentage. These data are supported by the biparametric analysis with Annexin V and PI.
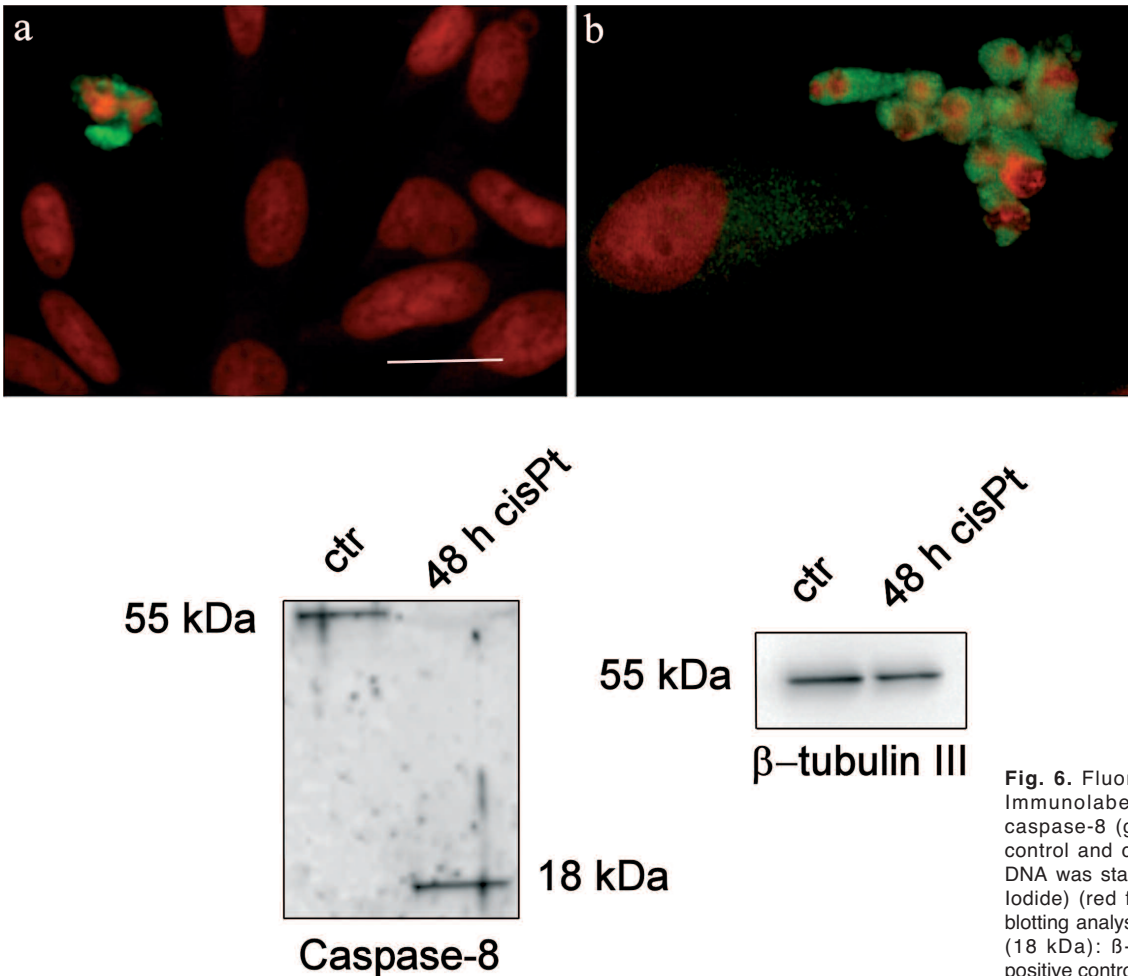

Fig. 6. Fluorescence microscopy. Immunolabelling for activated caspase-8 (green fluorescence) in control and cisPt treated B50 cells. DNA was stained with PI (Propidium Iodide) (red fluorescence). Western blotting analysis of cleaved caspase-8 (18 kDa): ß-tubulin III is used as positive control. Bar: 20 *μ*m.

Data from literature reported that cisPt induces the mitochondria-mediated death in different cell lines (Park et al., 2002; Kim et al., 2003; Bottone et al., 2008). This pathway includes both a caspase-dependent and a caspase-independent apoptosis, through the release of cytochrome c (Liu et al., 1996) and AIF (Susin et al., 1996), respectively.

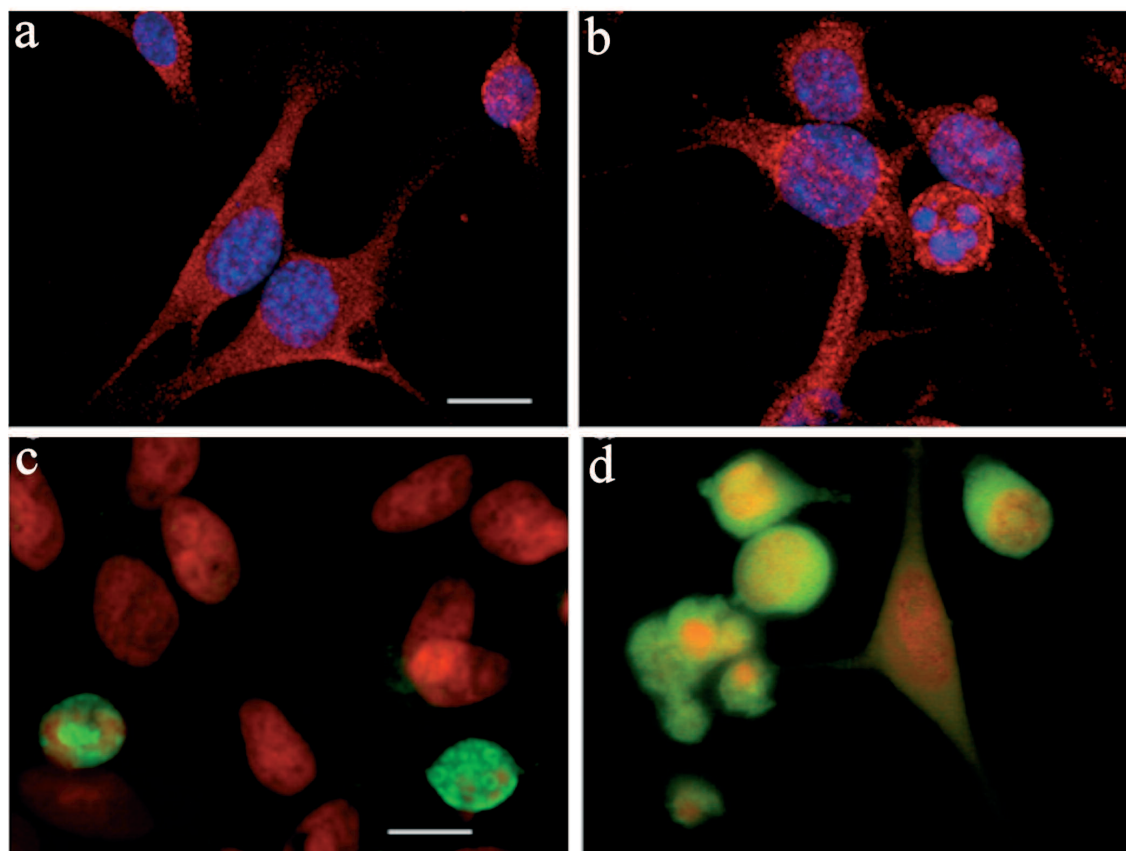Recently, Scovassi et al. (2009) demonstrated, in late

Fig. 7. Confocal microscopy. **a, b.** Endoplasmic reticulum immunolabelling (red fluorescence) in B50 cells: in untreated cells **(a)**, the cisternae of endoplasmic reticulum are distributed like a network around the nucleus; in cisPt treated cells **(b)** the cisternae form dense masses in the cytoplasm. DNA was stained with Hoechst 33258 (blue fluorescence). **c, d.** Fluorescence microscopy. Immunolabeling for active caspase-12 in control **(c)** and in cisPt treated **(d)** B50 cells (green fluorescence), DNA was stained with (Propidium Iodide) (red fluorescence). Western blotting analysis for cleaved caspase-12 (43 kDa): ß-tubulin III is used as positive control.
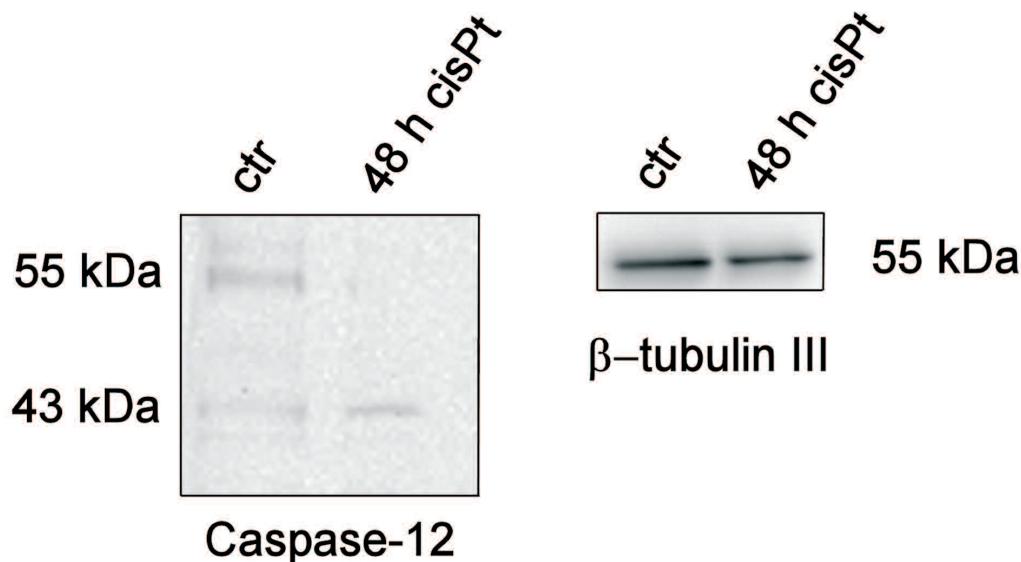
apoptotic HeLa cells, that AIF immunolabelling disappears from the nuclei, but it can be observed in the mitochondria and in the cytoplasm. Bottone et al. (2009) have hypothesized that AIF could be degraded during the late apoptotic phases or it could be synthesized de novo in the mitochondria.
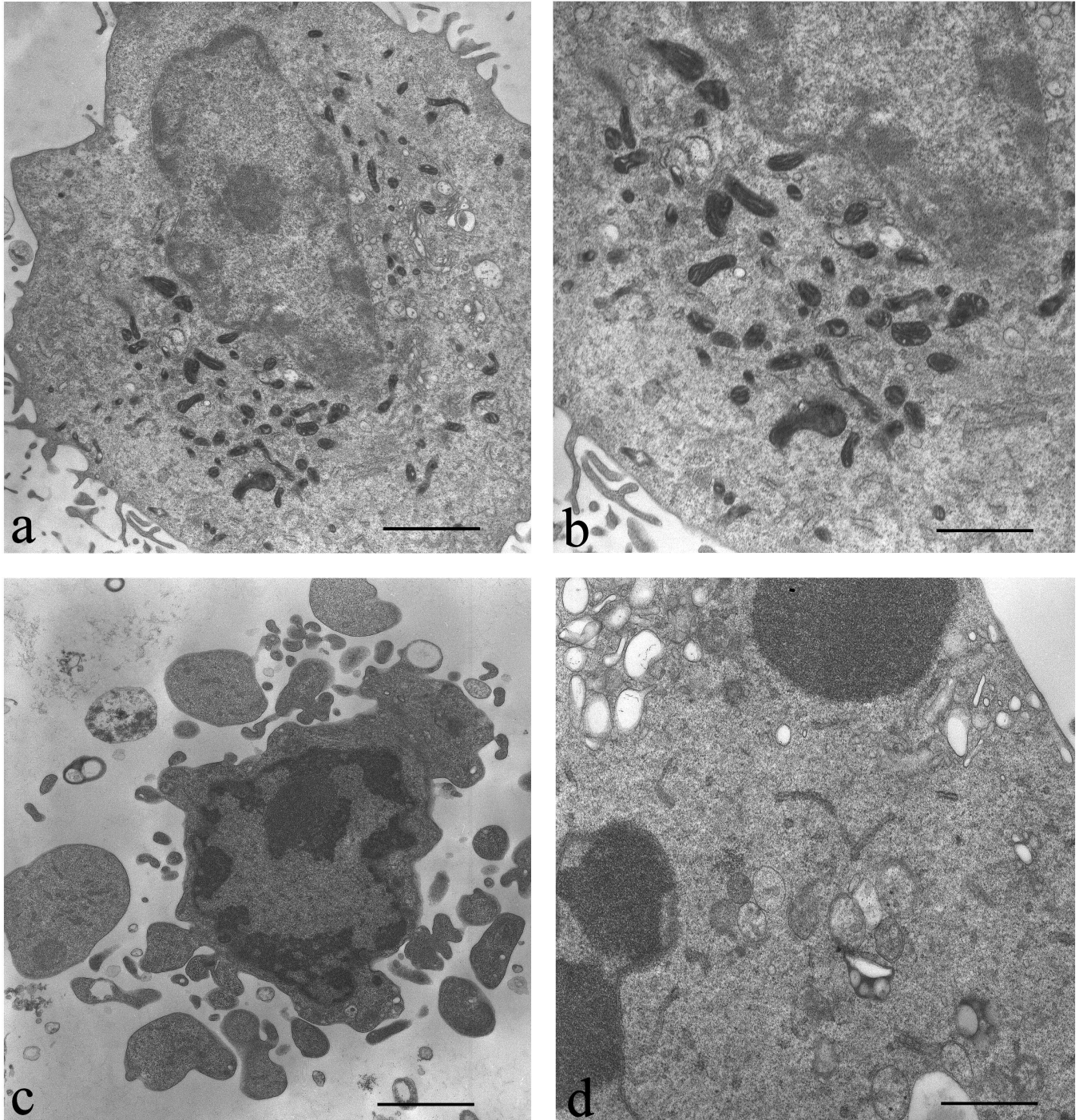

Fig. 8. Morphology of endoplasmic reticulum at transmission electron microscope. **a.** Untreated control. **b.** Untreated control. Star: physiological ER distribution. **c.** Cells treated with 48 h cisPt. **d.** Cells treated with 48 h cisPt. Arrows: altered ER distribution. Bars: a, c, 1.1 μm; b, d, 0.6 μm.
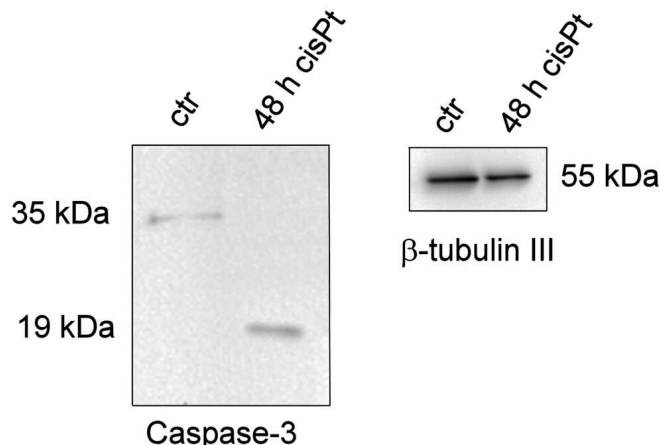
Fig. 9. Western blotting analysis of cleaved caspase-3 (19 kDa): ß-tubulin III is used as positive control.

Some evidence suggests, however, that a redox-active enzymatic region of AIF may be antiapoptotic, while a DNA binding region is pro-apoptotic (Lipton and Bossy-Wetzel, 2002).

Our results show that in early apoptotic B50 cells AIF locates in the nucleus, while in late apoptotic cells no signal for AIF was recorded in the Hoechst-stained nuclear fragments. Moreover, western blotting analysis indicates that AIF in control samples appears located at mitochondria, but after 48 h it disappears and relocates at the cytoplasm and nucleus. Other drugs, used on HeLa cells, induce the same relocalization of AIF (Scovassi et al., 2009). Western blotting experiment also confirms the release of cytochrome c from mitochondria to the cytoplasm during apoptosis.

Our results, both in immunocytochemistry and in western blotting, demonstrated that caspase-8 is activated in cisPt-induced apoptosis. According to studies of receptor-mediated apoptosis, activation of caspase-8 is the earliest event in the caspase cascade, which sequentially activates Apaf-1, caspase-9 and caspase-3 (Fulda, 2009).

Another apoptotic pathway considered is the one involving ER stress. *In vivo* studies suggested that, in some cases, ER stress may be tightly correlated with neurodegeneration, even if it may not be the primary cause of neuron death (Lindholm et al., 2006). Our results, obtained with cisPt treated B50 cells, demonstrated the link between ER stress and caspase-12 cleavage resulting in apoptosis.

The cleavage of caspase-12 and caspase-8 precedes the cleavage of the executioner caspase-3. Also, in this case, western blotting analysis confirms the activation, through cleavage, of caspase 3. Therefore, the apoptotic program represents a promising strategy, both to directly trigger programmed cell death in cancer cells and to sensitize cells for apoptotic stimuli in combination therapies.

References

Abraham M.C. and Shaham S. (2004). Death without caspases, caspases without death. Trends Cell Biol. 14, 184-193.

Adams J.M. (2003). Ways of dying: multiple pathways to apoptosis. Genes Dev. 17, 2481-2495.

Barnhart B.C., Lee J.C., Alappat E.C. and Peter M.E. (2003). The death effector domain protein family. Oncogene 22, 8634-8644.

Bodenner D.L., Dedon P.C., Keng P.C., Katz J.C. and Borch R.F. (1986). Selective protection against cis-diamminedichloro-platinum(II)-induced toxicity in kidney, gut, and bone marrow by diethyldithiocarbamate. Cancer Res. 46, 2751-2755.

Bottone M.G., Soldani C., Veneroni P., Avella D., Pisu M. and Bernocchi G. (2008). Cell proliferation, apoptosis and mitochondrial damage in rat B50 neuronal cells after cisplatin treatment. Cell Prolif. 41, 506-520.

Bottone M.G., Soldani C., Fraschini A., Croce A.C., Bottiroli G., Camboni T., Scovassi A.I. and Pellicciari C. (2009). Enzyme-assisted photosensitization activates different apoptotic pathways in Rose Bengal acetate treated Hela cells. Histochem. Cell Biol. 131, 391-399.

Bottone M.G., Giansanti V., Veneroni P, Scovassi A.I., Bernocchi G. and Pellicciari C. (2010). The apoptosis-inducing factor (AIF) moves from mitochondria to the nucleus and back to the cytoplasm, during apoptosis. In: Mitochondria: Structure, functions and dysfunctions. Svensson O.L. (ed). Nova Science Publishers, Inc. pp 11788-3619.

Camins A., Pallas M. and Silvestre J.S. (2008). Apoptotic mechanisms involved in neurodegenerative diseases: experimental and therapeutic approaches. Methods Find. Exp. Clin. Pharmacol. 30, 43-65.

Cece R., Barajon I. and Tredici G. (1995). Cisplatin induces apoptosis in SH-SY5Y human neuroblastoma cell line. Anticancer Res. 15, 777-782.

Dietrich J., Han R., Yang Y., Mayer-Pröschel M. and Noble M. (2006). CNS progenitor cells and oligodendrocytes are target of chemotherapeutic agents *in vitro* and *in vivo*. J. Biol. 5, 22.

Ferri K.F. and Kroemer G. (2001). Organelle-specific initiation of cell death pathways. Nat. Cell Biol. 3, 255-263.

Fisher D.E. (1994). Apoptosis in cancer therapy: Crossing the threshold. Cell 78, 539-542.

Fulda S. (2008). Caspase-8. In: Encyclopedia of cancer. Schwab M. (ed). Springer. Berlin.

Fulda S. (2009). Caspase-8 in cancer biology and therapy. Cancer Lett. 281, 128-133.

Kaufmann S.H. (2007). The intrinsic pathway of apoptosis. In: Apoptosis, senescence, and cancer. Gewirtz D.A., Grant S. and Holt S.E. (eds). Humana Press. pp 3-30.

Kim J.S., Lee J.M., Chwae Y-J., Kim Y.H., Lee J.H., Kim K., Lee T.H., Kim S.J. and Park J.H. (2003). Cisplatin-induced apoptosis in Hep3B cells: mitochondria-dependent and independent pathways. Biochem. Pharmacol. 67, 1459-1468.

Kruiderin G. and Evan G.I. (2000). Caspase-8 in Apoptosis: The Beginning of "The End"?. IUBMB Life 50, 85-90.

Lindholm D., Wootz H. and Korhonen L. (2006). ER stress and

neurodegenerative diseases. Cell Death Differ. 13, 385-392.

Lipton S.A. and Bossy-Wetzel E. (2002). Dueling activities of AIF in cell death versus survival: DNA binding and redox activity. Cell 111, 147-150.

Liu X., Kim C.N., Yang J., Jemmerson R. and Wang X. (1996). Induction of apoptotic program in cell-free extracts: requirement for dATP and cytochrome c. Cell 86, 147-157.

Modjtahedi N., Giordanetto F., Madeo F. and Kroemer G. (2006). Apoptosis inducing factor: vital and lethal. Trends Cell Biol. 16, 264-272.

Nakagawa T., Zhu H., Morishima N., Li E., Xu J., Yankner B.A. and Yuan J. (2000). Caspase-12 mediates endoplasmic-reticulum-specific apoptosis and cytotoxicity by amyloid-beta. Nature 403, 98-103.

Park M.S., De Leon M. and Devarajan P. (2002). Cisplatin induces apoptosis in LLC-PK1 cells via activation of mitochondrial pathways. J. Am. Soc. Nephrol. 13, 858-865.

Perier C., Bové J., Dehay B., Jackson-Lewis V., Rabinovitch P.S., Przedborski S. and Vila M. (2010). Apoptosis-inducing factor deficiency sensitizes dopaminergic neurons to parkinsonian neurotoxins. Ann. Neurol. 68, 184-192.

Rao R.V., Ellerby H.M. and Bredesen D.E. (2004). Coupling endoplasmic reticulum stress to the cell death program. Cell Death Differ. 11, 372-380.

Rosenberg B. (1999). Platinum complexes for the treatment of cancer: Why the search goes on, in Cisplatin. In: Chemistry and biochemistry of a leading anticancer drug. Lippert B. (ed). Wiley-VCH. Basel. pp 3-27.

Scovassi A.I., Soldani C., Veneroni P., Bottone M.G. and Pellicciari C. (2009). Changes of mitochondria and relocation of the apoptosis-inducing factor during apoptosis. Ann. NY Acad. Sci. 1171, 12-17.

Susin S.A., Zamzami N., Castedo M., Hirsch T., Marchetti P., Macho A., Daugas E., Geuskens M. and Kroemer G. (1996). Bcl-2 inhibits the mitochondrial release of an apoptogenic protease. J. Exp. Med. 184, 1331-1342.

Zhang Y., Zhang C., Narayani N., Du C. and Balaji K.C. (2007). Nuclear translocation of apoptosis inducing factor is associated with cisplatin induced apoptosis in LNCaP prostate cancer cells. Cancer Lett. 255, 127-134.